RSC Advances

PAPER

View Article Online
View Journal | View Issue

Cite this: *RSC Adv.*, 2020, **10**, 28213

Optical properties of 3-substituted indoles†

Jagdeep Kumar, Naresh Kumar and Prasanta Kumar Hota *

Received 20th June 2020
Accepted 23rd July 2020

DOI: 10.1039/d0ra05405d

rsc.li/rsc-advances

The optical properties of various donor or acceptor *p*-phenyl substituted ethenyl indoles were studied in solvents of varying polarity using absorption, fluorescence and TDDFT methods. Ethenyl indole exhibits non-linear optical properties (NLO) in a substituent dependent manner. Compound with a strong electron-attracting substituent, shows large NLO properties with charge transfer behavior, whereas ethenyls with moderate electron withdrawing or electron donating substituent exhibit lower NLO properties with non polar excited state. A highly dipolar excited state for *p*-nitro phenyl substituted ethenyl indoles (μ_e: 18.2–27.1 debye; $\Delta\mu$: 9.4–17.8 debye) is observed as compared to other ethenyls (μ_e: 6.6–9.5 debye; $\Delta\mu$: 4.2–6.2 debye). From TDDFT study, it is shown that the HOMO–LUMO energy of ethenyl is increased with increasing the electron donating ability of the *p*-phenyl substitution. The optical band gap of ethenyl **3** without substitution, is decreased upon *p*-phenyl substitution either with an electron withdrawing (Cl, NO_2) or an electron donating (OCH_3, OH, NH_2) substituent. The compound with a strong electron accepting, *p*-nitrophenyl ethenyl indole **1** shows 12 times better NLO response as compared to the reference ethenyl indole **3** (β: **1**: 115 × 10^{-30} esu^{-1} cm^5, **3**: 9 × 10^{-30} esu^{-1} cm^5). Ethenyls **2–6** bearing a weak or moderately electron withdrawing or electron accepting substituent, exhibit lower NLO response. The β of ethenyl is increased with increasing the order of electron withdrawing nature of phenyl ring. Overall, a correlation of β with the optical band gap, ground state dipole moment, % of charge transfer in the ground and excited state is found.

1. Introduction

Donor–acceptor substituted conjugated molecules have a wide range of applications in chemistry, biology[1–6] and organic electronics[7,8] like photoswitches,[9–12] organic light-emitting diodes (OLEDS),[13,14] dye-sensitized solar cell (DSSC),[15–25] nonlinear optics (NLO).[7,13,14,26–37] In particular, NLO materials with varied shape and size (*e.g.* dipolar, quadrupolar, octupolar) were developed and extensively studied using various testing methods such as electric field induced second harmonic (EFISH) generation, hyper Rayleigh scattering (HRS),[26–37] solvatochromic methods[38–46] and computational based density functional theory (DFT).[39,42] Among all the methods, the solvatochromic method is most suitable, easy and cost effective method, in which the NLO response, first hyperpolarizability coefficient (β) of small dipolar molecule can be obtained accurately.[38–46] The large second order NLO response, first hyperpolarizability can be achieved through extended conjugation as well as by tuning the donor–acceptor length in electron donor–acceptor substituted molecule.[7,8] NLO response of 6-substituted indole derivatives were tested previously.[47,48] These includes indole with tricyano furan acceptor based conjugated molecules and studied their thermal and electro-optic properties. It is shown that indole can act as a donor in developing nonlinear optical material. In such system, increasing the electron donating ability of indole moiety leads to decrease in thermal stability and increased in NLO responsive electro-optical properties.[47] Similarly, as compared to aniline, the 6-(pyrrolidin-1-yl)-1*H*-indole based donor system exhibits enhance in its macro NLO response electro-optic properties.[48] In such system, the NLO properties is increased with increasing the electron donating ability of indole moiety. This could be due to favorable intermolecular dipole interaction forces.[49] In comparison to earlier report, the 3-substituted indole derivatives are more sensitive to medium polarity due to (i) the formation of stable resonating structure at indolyl-3-position and (ii) the donating ability of indole moiety can also be tuned through various *N*-substitution.[50,51]

The advantage of these molecules is due to their substituent induced varied optical properties such as absorption, fluorescence, extinction coefficient, HOMO–LUMO energy gap, excited state dipole moment and transition energy, which provide most valuable information in designing future molecules. In order to gain more insight into the NLO response of 3-substituted indole based conjugated molecules, we have studied the substituent dependent first hyperpolarizability (β) of various electron donor/acceptor substituted *p*-phenyl and *N*-substituted ethenyl indoles (**1–9**) using solvatochromic method. The ethenyls (**1–9**) with varied electron withdrawing and donating *p*-phenyl substitution (NO_2, Cl, H, OCH_3, OH, NH_2, N–$SO_2C_6H_5$, N–

Department of Chemistry, School of Sciences, Hemvati Nandan Bahuguna Garhwal University, Srinagar (Garhwal), Uttarakhand 246174, India. E-mail: p.hota@hnbgu.ac.in

† Electronic supplementary information (ESI) available. See DOI: 10.1039/d0ra05405d

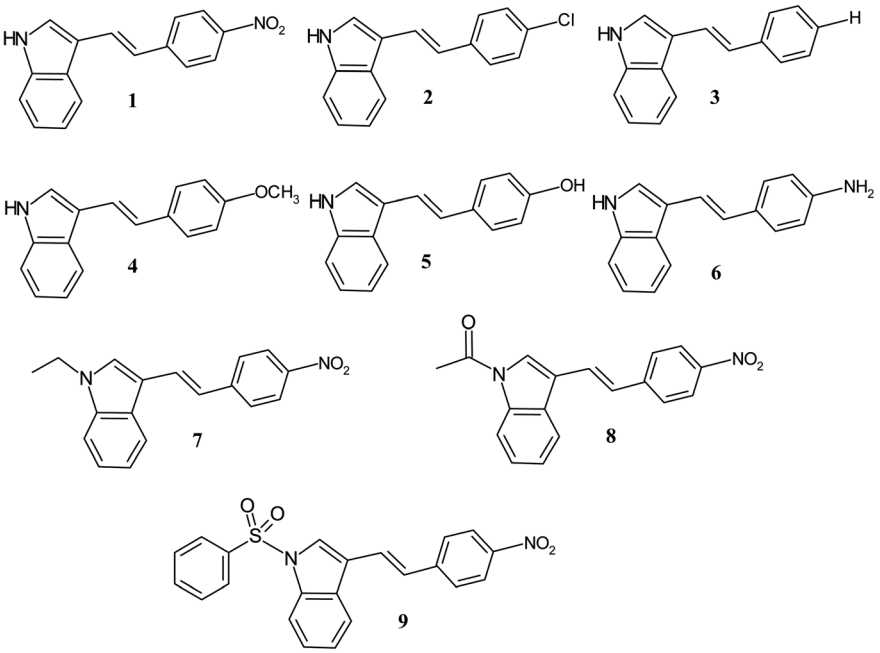

Scheme 1 Structure of indole compounds **1–9**.

$COCH_3$, N–Et) were synthesized (Scheme 1) and the effect of substitution on the optical properties of indole compounds were evaluated.

The excited state of nitro substituted ethenyls (**1**, **7**, **8**, **9**) is highly dipolar and exhibit charge transfer excited state. A higher β value is found for these ethenyls bearing a strong electron withdrawing substituent. On the other hand, excited state of compounds **2–6** is non-polar and exhibit a lower β value. Overall, the 2nd order NLO properties is proportional to the ground state dipole moment, polarizability, ionic character and % of charge separation in the molecule. On the other hand, β value is inversely proportional to the optical band gap of the ethenyl indole. The above substituent dependent studies on *p*-phenyl and *N*-substituted ethenyl indole provide most valuable information in understanding the optical properties in conjugated molecules.

2. Experimental section

2.1 Materials and analytical equipments

The starting materials and reagents for the synthesis of ethenyl indoles were purchased from the local suppliers (Ms E. Merck, Sisco Research Laboratory, Sigma-Aldrich). UV grade solvents are used for spectroscopy study. Compounds are synthesized using Carousel 6 plus reaction station, Radleys make. Synthetic compounds are characterized by ^{1}H and ^{13}C nuclear magnetic resonance (NMR), Fourier-transform infrared (FTIR), mass spectrometry (MS) using electron impact (EI) method and carbon, hydrogen, nitrogen and sulfur (CHNS) analysis. The absorption spectra are recorded on a PerkinElmer Lambda 25 UV-Vis and Lambda 750 UV/VIS/near infrared (NIR) spectrophotometer. The fluorescence spectra are recorded on a PerkinElmer LS-55 fluorescence spectrophotometer using a red photomultiplier tubes (PMT) detector system. FTIR spectra are recorded on a Impact Nicolet-400 spectrophotometer using KBr discs. The ^{1}H and ^{13}C NMR spectra are recorded on a JEOL 500 MHz FTNMR instrument in $CDCl_3$ as solvent and using tetramethylsilane (TMS) as an internal standard. MS spectra are measured on a GCD 1800A Hewlett Packard gas chromatography (GC)–mass spectrometer. CHNS analyses are recorded on a Theoquest CE instrument 1112 series CHNS auto analyzer. Melting points are recorded on a Lab India make melting point apparatus.

2.2 Synthesis of compounds 1–9

The substituted *p*-phenyl ethenyl-*E*-indoles (**1–5**) are synthesized through condensation of 2 molar ratio of *p*-substituted phenyl acetic acid with respect to 3-formylindole in pyridine–piperidine mixture as described earlier[6,45,46,50,51] and the routes are shown in Scheme 2, *e.g.* for obtaining compound **1**, the typical synthetic protocol is as follows: 2-formyl indole (1.45 g, 0.01 M) is taken with *p*-nitrophenyl acetic acid (3.62 g, 0.02 mol) along with in freshly distilled pyridine (10 mL) and piperidine (0.6 mL) in a round bottom flask. The reaction mixture was refluxed at 100 °C for six hours. The progress of the reaction is monitored by thin layer chromatography (TLC). After cooling the reaction mixture, the excess of pyridine was remove from the reaction mixture by treating with 100 mL of diluted hydrochloric acid. A red colored product is collected after extracting the crude product in dichloromethane. The product was further purified by column chromatography using 2% ethyl acetate in petroleum ether as the eluting solvent. The yield of the desired compound is obtained in 31%. Similarly, compounds **2–5** were obtained with yield 56%, 45%, 34% and 33% respectively. Compound **6** was prepared with 47% yield through reduction reaction of **1**. For this purpose, the

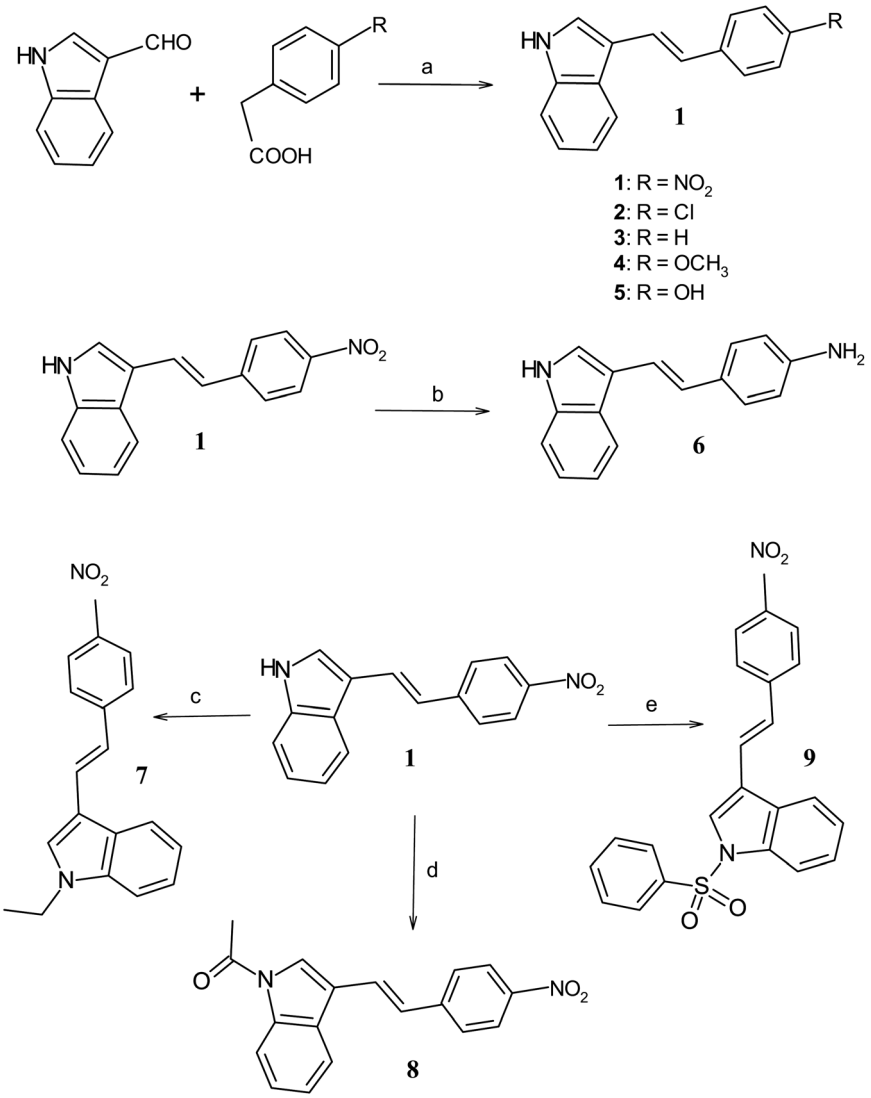

Scheme 2 Synthetic routes and reaction conditions for obtaining indole compounds, (a) pyridine, piperidine, 100 °C, reflux, 6 h; (b) $FeSO_4$, aqu. NH_3, ethanol, 100 °C, 3 h; (c) ethyl bromide, potassium-*t*-butoxide, *t*-butyl alcohol, reflux, 4 h; (d) acetic anhydride, sodium acetate, reflux, 1 h; (e) benzene sulphonyl chloride, potassium carbonate, acetone, 0 °C, 2 h.

alcoholic solution of ethenyl indole **1** (0.2 g, 0.001 M) is refluxed in ferrous sulfate (1.5 g, 0.01 M) and aqueous ammonia solution at 100 °C for 3 h. Compound **7** was obtained with 80% yield through *N*-alkylation of compound **1** (0.5 g, 0.002 M) with ethyl bromide (2 mL, 0.01 mol) in presence of potassium-*t*-butoxide (0.2 g, 0.002 M) and *t*-butyl alcohol (20 mL).[52] Compound **8** was obtained with 83% yield through *N*-acetylation of compound **1** (0.1 g, 0.0004 M) using acetic anhydride (10 mL) in presence of sodium acetate (0.1 g, 0.0012 M).[53] Compound **9** was obtained with 80% yield through *N*-sulphonation of compound **1** (0.2 g, 0.001 M) using benzene sulphonyl chloride (1 mL, 0.01 M) and potassium carbonate (1.0 g, 0.01 M) in acetone[54] as shown in Scheme 2. The products are purified by column chromatography using 2–5% ethyl acetate in petroleum ether (60–80 °C) as the eluting solvent. The characterization of compounds were carried out satisfactory using ^{1}H and ^{13}C NMR, MS, FTIR, CHNS analysis.

2.3 Absorption and fluorescence studies

For all absorption and fluorescence measurements, UV grade solvents were used. For absorption, (1–4) $\times$ 10^{-5} M solution and for fluorescence studies, 0.5 $\times$ 10^{-5} M solution of compounds were prepared in different solvents and recorded using a 1 cm $\times$ 1 cm, light path length quartz cuvette. Fluorescence spectra were recorded by exciting the sample at their absorption maximum ($\lambda_{abs\ max}$). The ground and excited state energy (E) of the compounds are calculated using absorption wavelength ($\lambda_{abs\ max}$), fluorescence wavelength ($\lambda_{em\ max}$) maximum and eqn (1). Where,

$$E_{abs} = (hc/\lambda_{abs\ max}) = (1.24/\lambda_{abs\ max}) \text{ (in KeV)} \quad (1a)$$

$$E_{em} = (hc/\lambda_{em\ max}) = (1.24/\lambda_{em\ max}) \text{ (in Kev)} \quad (1b)$$

The energy band gap (ΔE) of **1–9** is obtained from the intersection of excitation and fluorescence spectrum, Tauc plot and TDDFT computation method.

2.4 Dipole moment calculation

Change of excited state dipole moment of compounds is calculated using McRay eqn (2).[41,55]

Table 1 UV-Vis absorption and fluorescence data of **1–9** in different solvents

	Solvents	$\lambda_{abs\ max}$ (nm)	ε (M^{-1} cm^{-1})	$\lambda_{em\ max}$ (nm)	$\lambda_{ex\ max}$ (nm)	Stokes' shift ($\nu_a - \nu_f$) nm (cm^{-1})	Quantum yield Φ_f
1	*n*-Hexane	403	15 423	497	408	94 (4693)	0.0104
	1,4-Dioxan	407	21 011	554	372	147 (6520)	0.0216
	THF	416	22 603	607	443	191 (7564)	0.0418
	MeOH	413	23 900	590	370	177 (7264)	0.0013
	AcCN	411	24 924	642	380	231 (8754)	0.0118
	DMF	427	17 068	648	446	221 (7987)	0.0052
2	*n*-Hexane	338	17 900	384	351	46 (3544)	0.0026
	1,4-Dioxan	336	14 750	388	341	52 (3988)	0.0037
	THF	333	18 600	387	345	54 (4191)	0.0020
	MeOH	335	18 800	395	354	60 (4534)	0.0016
	AcCN	340	19 475	396	355	56 (4159)	0.0015
	DMF	338	18 075	398	350	60 (4460)	0.0024
3	*n*-Hexane	328	4675	384	335	56 (4446)	0.0066
	1,4-Dioxan	329	14 575	384	325	55 (4354)	—
	THF	331	14 200	397	347	66 (5023)	0.0083
	MeOH	327	10 800	396	323	69 (5329)	0.0072
	AcCN	325	14 925	407	333	82 (6199)	—
	DMF	332	14 975	404	346	72 (5368)	0.0110
4	*n*-Hexane	328	15 496	389	340	61 (4781)	0.0027
	1,4-Dioxan	330	18 229	397	329	67 (5115)	0.0209
	THF	331	17 101	403	324	72 (5398)	0.0163
	MeOH	327	17 800	404	344	77 (5829)	0.0137
	AcCN	326	15 020	409	349	83 (6225)	0.0176
	DMF	333	18 530	411	349	78 (5700)	0.0196
5	*n*-Hexane	310	14 987	389	308	79 (6552)	0.0114
	1,4-Dioxan	318	18 333	384	330	66 (5405)	0.0035
	THF	319	21 754	385	332	66 (5373)	0.0058
	MeOH	322	24 400	390	330	68 (5414)	0.0030
	AcCN	323	16 741	395	335	72 (5643)	0.0042
	DMF	331	15 588	398	347	67 (5086)	0.0081
6	*n*-Hexane	320	8467	389	333	69 (5544)	0.0361
	1,4-Dioxan	324	14 522	394	354	70 (5484)	0.0041
	THF	325	2989	397	355	72 (5581)	0.0334
	MeOH	324	12 200	405	339	81 (6173)	0.0301
	AcCN	325	12 814	397	337	72 (5581)	0.0745
	DMF	333	12 185	400	365	67 (5030)	0.0056
7	*n*-Hexane	402	24 026	508	395	106 (5190)	0.0005
	1,4-Dioxan	415	27 090	566	406	151 (6429)	0.0006
	THF	420	23 141	590	420	170 (6860)	0.0007
	MeOH	415	22 823	556	417	141 (6111)	0.0006
	AcCN	419	21 238	649	415	230 (8482)	0.0008
	DMF	430	27 318	640	426	210 (7630)	0.0007
8	*n*-Hexane	362	13 975	423	363	61 (3984)	0.0003
	1,4-Dioxan	378	12 655	533	370	155 (7694)	0.0007
	THF	375	11 800	537	375	162 (8045)	0.0008
	MeOH	375	11 464	564	374	189 (8936)	0.0009
	AcCN	376	10 900	602	374	226 (9984)	0.0010
	DMF	382	11 200	592	380	220 (9287)	0.0009
9	*n*-Hexane	360	26 722	403	356	43 (3197)	0.0003
	1,4-Dioxan	369	27 742	529	371	160 (8196)	0.0008
	THF	374	16 773	576	377	202 (9376)	0.0008
	MeOH	370	20 000	588	371	218 (10 020)	0.0009
	AcCN	369	14 065	593	370	224 (10 236)	0.0010
	DMF	377	14 178	605	369	228 (9996)	0.0009

$$\nu_{abs} - \nu_{em} = (\delta_{abs} + \delta_{em}) + \{(2\Delta\mu^2/hca^3)F(\varepsilon,n)\} = \text{constant} + mF(\varepsilon,n) \quad (2)$$

$$F(\varepsilon,n) = [(\varepsilon - 1)/(\varepsilon + 2) - (n^2 - 1)/(n^2 + 2)],\ m = (2\Delta\mu^2/hca^3)$$

where, ν_{abs} is absorption maximum wave number, ν_{em} fluorescence maximum wave number, $\nu_{abs} - \nu_{em}$ is the Stokes' shift, δ_{abs} and δ_{em} are difference in vibrational energy of molecule (in cm^{-1}) in excited and ground state for absorption and emission respectively, μ_e and μ_g are the excited state and ground state dipole moments respectively, $\mu_e - \mu_g = \Delta\mu$ is the change in dipole moment, h is the Planck constant (6.62×10^{-34} joule s), c is the velocity of light in vacuum (3×10^8 meter per s), ε is the relative permittivity (*i.e.* dielectric constant) and n is the refractive index of the solvent.[56,57] The Onsagar cavity radius (a) can be calculated using eqn (3) as described elsewhere.[58]

$$a = (3M/4\pi\delta N)^{1/3}, \quad (3)$$

where, M = molecular weight of molecule, N = Avogadro number = 6.022×10^{23}, δ = molecular density of molecule.

2.5 First hyperpolarizability calculation

The first hyperpolarizability coefficient (β) is related to second order nonlinear optical (NLO) properties of molecule. The solvatochromism method is used to obtain β in methanol using Oudar formula[59] as reported elsewhere[38–44] using eqn (4) and eqn (5).

$$(\beta) = (3/2h^2c^2) \times \{(\nu_{abs})^2(r_g)^2(\Delta\mu)\}/\{(\nu_{abs}{}^2 - \nu^2)(\nu_{abs}{}^2 - 4\nu^2)\} \quad (4)$$

where, ν_{abs}: absorption maximum wave number and; ν: incident reference wave number, 1064 nm of Nd:YAG laser source to which the β value is referred;

The transition dipole moment (r_g) is calculated using eqn (5).

$$(r_g)^2 = [(3e^2h)/(8\pi^2mc)] \times (f/\nu_{abs}) = 2.13 \times 10^{-30} \times (f/\nu_{abs}) \quad (5)$$

where, f is the Oscillator strength, $f = 4.32 \times 10^{-9} \int \varepsilon(\nu)d\nu$, which is obtained from the plot, molar absorption coefficient (ε) *vs.* wave number (ν).[60]

2.6 Computed parameters using time dependent density functional theory (TDDFT)

For computational calculation, the Orca quantum chemical software package[61–63] with time dependent density functional theory (TDDFT)[64–66] is used. The ground state dipole moment, absorption wavelength, the vertical excitation energy, oscillator strength of the optimized ethenyls were obtained using B3LYP functional with a def2 SVP basis set.[67]

3. Results and discussion

3.1 Synthesis

The *trans*-olefins of **1–9** were obtained through condensation reaction as shown in Scheme 2 with reasonable yield (31–83%). Overall the yield of reaction is obtained satisfactory. All the compounds were characterized through ^{1}H NMR, ^{13}C NMR, FTIR, MS (EI + method) and CHN analysis. In ^{1}H NMR, the two doublet peaks correspond to *trans* olefin protons of compound **1–9** appear near δ 7.2 and δ 7.4 (each of 1H, J = 15.8–16.5 Hz). Similarly, multiplate peaks near δ 7.1–7.2 (2H, m $-C_5$–H, C_6–H), one singlet peak near δ 7.3–7.4 (1H, s, $-C_2$–H), two doublet peaks near δ 7.9 (1H, d, J = 7.5–8.2 Hz, $-C_4$–H) and δ 8.0 (1H, J = 6.2–7.5 Hz, $-C_7$–H) correspond to the indole ring protons. In FTIR, the indole N–Hst is identified near 3370 cm^{-1}. The C–Hst appear near 3040 cm^{-1}, C=Cst near 1620 cm^{-1}. Similarly, four peaks correspond to the C=Cst and C–Cst of phenyl ring are observed near 1520 cm^{-1}, 1488 cm^{-1}, 1455 cm^{-1}, 1400 cm^{-1}. For compound **1**, the symmetrical and asymmetrical stretching frequency of nitro group is confirmed at 1330 cm^{-1} and 1520 cm^{-1}. In compound **4**, the methoxy, O–Cst is confirmed at 1244 cm^{-1}. For compound **6**, two sharp peaks at 3394 cm^{-1} and 3341 cm^{-1} are confirmed as primary amine NHst. For compound **7–9**, the NHst peaks are disappeared upon *N*-substitution. For **8**, the C=O stretching peak at 1703 cm^{-1} correspond to *N*-acetyl group and for **9**, the S=O stretching appears at 1180 cm^{-1}. Thus, olefins bearing indole heterocyclic unit and indole *N*-substituted ethenyls were synthesized using mild reaction condition and characterized successfully. The detail of characterization data is shown in ESI.†

3.2 Absorption and fluorescence studies of indole compounds 1–9

The absorption and fluorescence data of compounds **1–9** in different solvents of varying polarity are summarized in Table 1. From the absorption (Fig. 1 and S1a-i†) and fluorescence spectra (Fig. 2 and S2a-i†), it is shown that the absorption coefficient of ethenyl indoles (**1–9**) is in between 10 800–23 900 M^{-1} cm^{-1} (Table 2). On increasing the solvent polarity, the absorption and fluorescence wavelength maximum are red shifted. This suggest, a π–π^* nature of electronic transition. On increasing the solvent polarity from *n*-hexane to

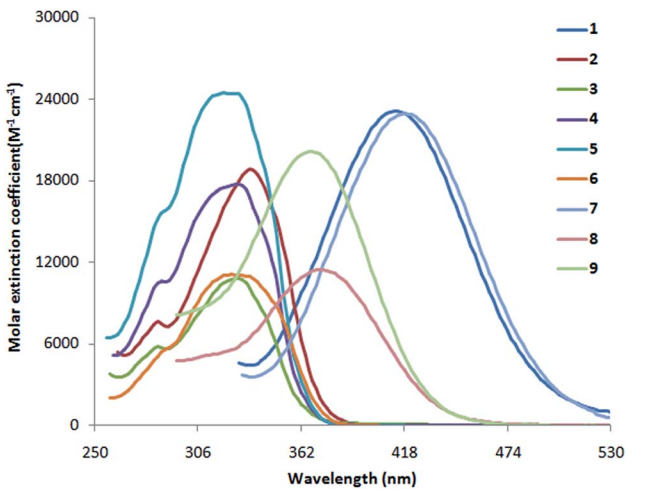

Fig. 1 Absorption spectra of **1–9** in methanol.

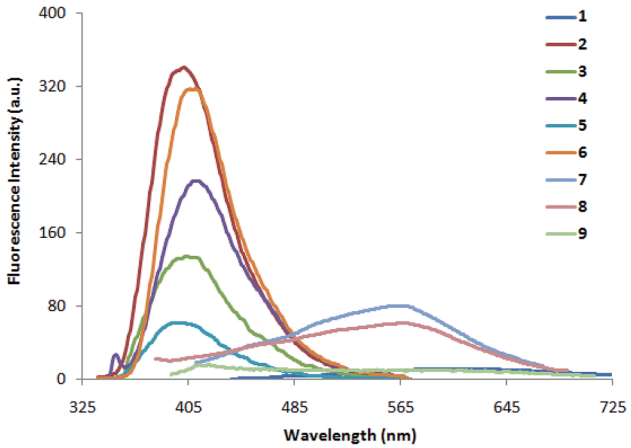

Fig. 2 Fluorescence spectra of **1–9** (0.5×10^{-5} M) in methanol.

dimethylformamide (DMF), the absorption maximum ($\lambda_{abs\ max}$) is moderately red shifted by 24 nm, 29 nm, 22 nm, 17 nm and 13 nm respectively for strong electron withdrawing nitro ethenyls (**1**, **7–9**) and for strong electron donating amino compound **6**. The $\lambda_{abs\ max}$ of compound **5** with phenolic group is also moderately red shifted by 11 nm from *n*-hexane to polar solvent, DMF. On the other hand, the $\lambda_{abs\ max}$ of other ethenyls **2–4** (Cl, H, OCH_3) is not much sensitive to solvent polarity and a red shift of 0–5 nm is observed. In contrast to $\lambda_{abs\ max}$, the fluorescence maximum ($\lambda_{em\ max}$) is significantly red shifted by 151 nm, 133 nm, 172 nm, 202 nm for **1**, **7–9** respectively from *n*-hexane to DMF. For **2–6**, $\lambda_{em\ max}$ is moderately red shifted by 14 nm, 20 nm, 22 nm, 09 nm and 11 nm respectively. This suggest the drastic stabilization of the excited state of **1**, **7–9** due to coulomb interaction between the dipolar solute and solvent molecules.[68,69] A red-shifted $\lambda_{em\ max}$ in ethenyl indole (**1**, **7–9**) is due to the electron delocalization from the indole moiety-to-the electron acceptor nitro group. As the transition is $\pi \rightarrow \pi^*$ nature, the more stabilization of excited state with respect to the ground state leads to a red shifted in absorption and fluorescence wavelength. From the correlation of Hammett substituent constant,[70] it is shown that strong electron acceptor $-NO_2$ group (σ_p +0.81, for **1**, **7–9**) at the *p*-phenyl ring induces large electron delocalization in the excited state as compared to the weak electron acceptor chloro group –Cl (σ_p +0.24, in case of **2**), –H (σ_p 0.0 in case of **3**) and weak electron donor methoxy group $-OCH_3$, (σ_p −0.28, in case of **4**).

The singlet state energy of **1–9** is calculated from their absorption and fluorescence wavelength maximum (Table 2). The first singlet excited state energy band gap for **1**, **7–9** is 2.47–2.87 eV, whereas it is 3.34–3.40 eV for **2–6**. As per Tauc plot and TDDFT calculation, the order is **3** > **2** > **9** > **8** > **1** > **2** and **3** > **4** = **5** > **6** (Fig. S3†). The optical band gap of **1** and **7–9** is 0.70–0.94 eV lower than compound **2–6**. Interestingly, indole is acting as a strong electron donor in presence of an electron withdrawing *p*-phenyl nitro substituent (for **1**, **7–9**), whereas indole acts as a weak electron acceptor in presence of an electron donating *p*-phenyl methoxy and amine (OCH_3, NH_2) substituent. In order to understand the effect of substituent and solvent polarity on the

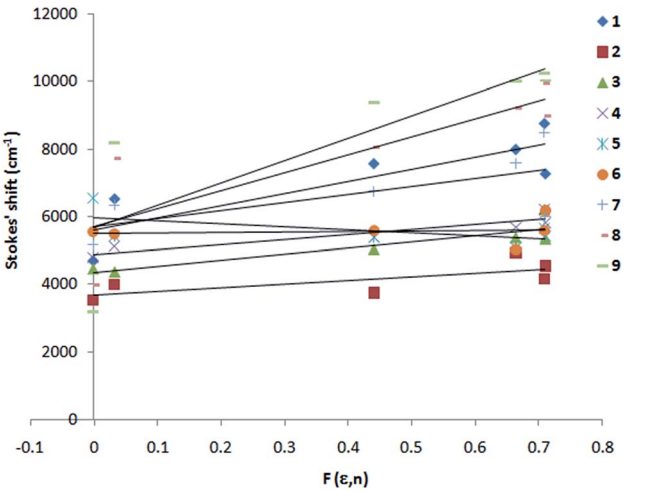

Fig. 3 McRay plot, Stokes' shift *vs.* $F(\varepsilon,n)$ of **1–9**. Solvents used are *n*-hexane, 1,4-dioxane, THF, MeOH, AcCN and DMF.

Table 2 Comparison of absorption wavelength maximum ($\lambda_{abs\ max}$), fluorescence wavelength maximum ($\lambda_{em\ max}$), extinction coefficient, oscillator strength (*f*), S_0–S_1 transition state energy (ΔE, eV), transient dipole moment between ground and excited states (r_g), change of excited state dipole moment ($\Delta\mu$), optical band gap (ΔE), first hyperpolarizability (β) of ethenyl indoles **1–9** in methanol[a]

	$\lambda_{abs\ max}$ (nm)	$\lambda_{em\ max}$ (nm)	(ε) (M^{-1} cm^{-1})	*f*	S_0–S_1 (ΔE) (eV)	(r_g) debye	($\Delta\mu$) debye	(μ_e) debye	(β) (in 10^{-30}) esu^{-1} cm^5
1	413	590	23 900	0.69	2.50	7.79	9.86	18.25	115
2	335	395	18 800	0.57	3.34	6.37	5.52	9.51	20
3	327	396	10 800	0.34	3.41	4.86	5.19	7.76	9
4	327	404	17 800	0.58	3.40	6.35	5.77	6.82	17
5	322	390	24 400	0.81	3.40	7.45	6.29	7.66	24
6	324	405	12 200	0.44	3.34	5.51	4.18	6.62	9
7	418	558	22 823	0.61	2.47	7.36	9.44	18.38	106
8	374	563	11 464	0.32	2.83	5.03	14.21	18.55	43
9	370	588	20 000	0.56	2.87	6.64	17.78	27.10	90

[a] Onsagar cavity radius "*a*" (in Å); **1**: 4.53; **2**: 4.47; **3**: 4.38; **4**: 4.55; **5**: 4.43; **6**: 4.45; **7**: 4.74; **8**: 4.75; **9**: 5.12; ground state dipole moment μ_g (in debye): **1**: 8.39; **2**: 3.99; **3**: 2.57; **4**: 1.05; **5**: 1.37; **6**: 2.44; **7**: 8.94; **8**: 4.34; **9**: 9.32; excited state dipole moment $\mu_e = \Delta\mu^{(McRay\ method)} + \mu_g^{(TDDFT)}$.

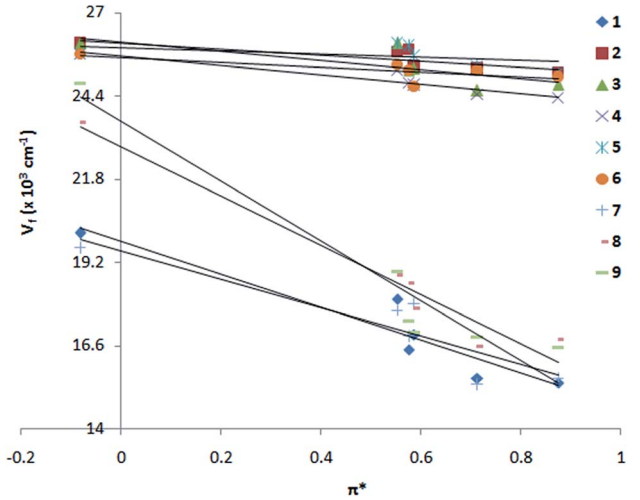

Fig. 4 Kamlet–Taft plot, emission wave number *vs.* solvent polarizability parameter π* of **1–9** in solvents, *n*-hexane, 1,4-dioxane, THF, MeOH, AcCN and DMF.

excited state, McRay plot, the Stokes' shift ($\nu_a - \nu_f$) *vs.* solvent polarity parameter, $F(\varepsilon,n)$ is drawn, (Fig. 3) for **1–9** and the excited state dipole moment is calculated (Tables 2 and S1†). For all compounds, the Stokes' shift values are increased linearly with increasing the solvent polarity. This further improved by the deletion of two solvents, 1,4-dioxan and acetonitrile. In order to get a good correlation factor, these two solvents were excluded from our calculation and the following correlation are obtained (**1**: $m_1 = 4245$, $R = 0.91$; **2**: $m_1 = 1384$, $R = 0.99$; **3**: $m_1 = 1304$, $R = 0.99$; **4**: $m_1 = 1434$, $R = 0.99$; **5**: $m_1 = -1847$, $R = 0.92$; **6**: $m_1 = 805$, $R = 0.85$; **7**: $m_1 = 3397$, $R = 0.92$, **8**: $m_1 = 7645$, $R = 0.97$, **9**: $m_1 = 9563$, $R = 0.95$). It is shown that a large change in the excited state dipole moment is observed for **1**, **7**, **8** and **9** (9.44–17.78 debye) as compared to **2**, **3**, **4**, **5** and **6** (4.18–6.29 debye). Similarly, the ground state dipole moment (μ_g) is computed for **1–9** using TDDFT. The μ_g for **2–6** is in between 1.05–3.99 debye, whereas μ_g for **1**, **7**, **8**, **9** is 4.34–9.32 debye (Table S1†). Thus, the large solvatochromic shift in **1** and **7–9** is due to charge transfer excited state. On the other hand, ethenyl indoles **2–6** with a weak electron acceptor or donor group (–Cl, –H, $-OCH_3$, –OH, $-NH_2$) show small change in excited state dipole moment (4.18–6.29 D) and exhibit non polar excited state as compared to **1** and **7–9**.

From Kamlet–Taft plot[71] (Fig. 4 and Table S1†), it is shown that nitro compounds (**1**, **7–9**) are highly polarized in the excited state. A large slope is observed for **1** and **7–9** as compared to **2–6** (slope: -5.14×10^{-3}, $R = 0.98$ for **1**; -0.93×10^{-3}, $R = 0.85$ for **2**; -1.32×10^{-3}, $R = 0.99$ for **3**; slope -1.43×10^{-3}, $R = 0.99$ for **4**; slope -2.69×10^{-3}, $R = 0.91$ for **5**; slope -0.71×10^{-3}, $R = 0.96$ for **6**; -4.03×10^{-3}, $R = 0.94$ for **7**; -7.38×10^{-3}, $R = 0.98$ for **8**; -9.22×10^{-3}, $R = 0.97$ for **9**). The formation of charge transfer excited state in **1** and **7–9** could be due to twist over the single bond attached to the *p*-phenyl ring and such phenomena is also suggested in other donor–acceptor substituted ethenyl systems.[45,46,72–79]

3.3 Time dependent density functional theory (TDDFT) studies

The geometry of the molecules are optimized and the parameters such as absorption, oscillator strength, HOMO–LUMO energy, optical band gap is computed for **1–9** using TDDFT method (Table S2†). The parameters obtained through computation methods are also followed the similar trend as compared to the experimental results. Compound with strong electron withdrawing *p*-phenyl substituent, the ground and excited states are stabilized, whereas, the ground and excited state are destabilized in presence of electron donating substituent compared to the unsubstituted ethenyl indole **3**. This is due to the pushing or pulling of π electrons from indole to the *p*-phenyl substituted ring, which leads to the stabilization or destabilization of the ground or excited state.

All these compounds show one intense band ($\lambda_{abs\ max}$ 300–440 nm). Compound **1** exhibits longest $\lambda_{abs\ max}$ of 434 nm and **3** has the lowest $\lambda_{abs\ max}$ of 341 nm. This absorption is due to the HOMO → LUMO ($S_0 \rightarrow S_1$) transition (Fig. S4†). From

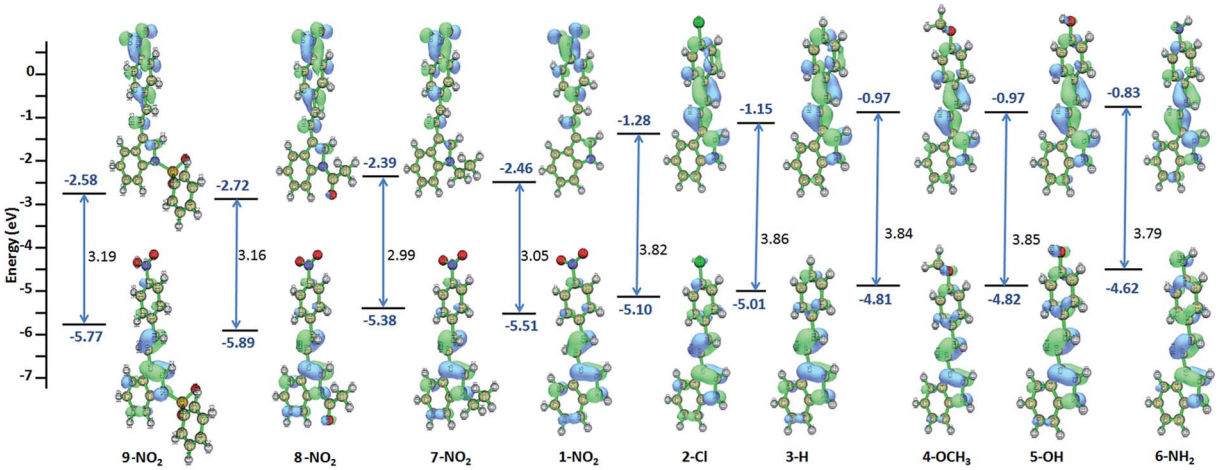

Fig. 5 TDDFT computed molecular orbitals, optical band gap and HOMO–LUMO energy of **1–9**.

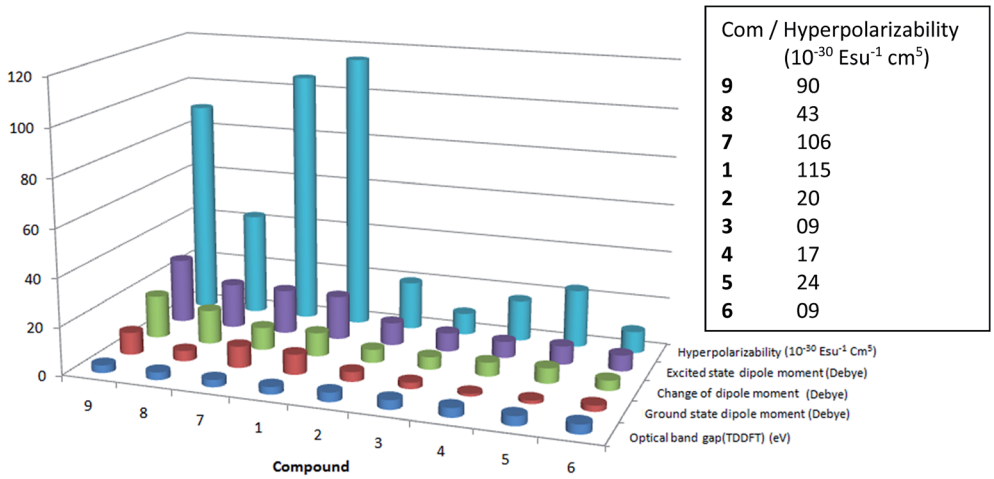

Fig. 6 Comparative chart of first hyperpolarizability (β_{CT}), excited state dipole moment, change of excited state dipole moment, ground state dipole moment and optical band gap of **1–9**.

solvatochromism data, these absorption is due to the $\pi \rightarrow \pi^*$ transition. As compared to, ethenyl indole (**3**), the HOMO–LUMO optical band gap is decreased upon increasing the electron withdrawing or electron donating *p*-phenyl substitution. The energy band gap is decreased by 0.81 eV from phenyl ethenyl indole (**3**) to *p*-nitro phenyl ethenyl indole (**1**) [3.85 eV (for 3) to 3.05 eV (for **1**)] (Fig. 5 and S5†). Similarly, the energy band gap is slightly decreased by 0.07 eV from phenyl ethenyl indole (**3**) to *p*-hydroxy phenyl ethenyl indole (**5**) [3.86 eV for **3** to 3.79 eV for **5**], whereas the band gap is comparable for amino and methoxy substituent [3.86 eV for **3** to 3.84 eV for **4**, 3.85 eV for **6**]. Interestingly, *N*-ethyl substitution destabilized the ground and excited state of **1**, whereas the ground and excited state is stabilized upon *N*-acetyl and *N*-sulfonyl substitution. Overall, the HOMO and LUMO energy of ethenyl indole, is progressively stabilized for electron withdrawing group due to the delocalization of π electron from indole to the *p*-phenyl ring (for NO_2, Cl) (Fig. S6†). In case of electron donating substituents (methoxy, hydroxy and amino) (**4–6**), the destabilization of HOMO and LUMO energy level could be due to the hindrance in effective π conjugation.

3.4 Second order non-linear optical properties

The first hyperpolarizability coefficient (β) is related to the second order non-linear optical properties of the molecule. Thus, β of the compounds **1–9** is calculated in solvent, methanol using solvatochromism method. In general, non linear optical properties of the molecule is influenced by the delocalization of π electron. Thus, the effect of *p*-phenyl and *N*-substitution on the NLO response of the ethenyl indole **3** is studied. For this purpose, the absorption, oscillator strength (f), dipole moment ($\Delta\mu$) and transition dipole moment (r_g) of the molecules were calculated. It is shown that as compared to the reference compound **3**, the β increases for strong electron withdrawing *p*-nitro phenyl substituent (Table 2, Fig. 6 and S7†). Compound **1** and **7–9**, which have strong electron withdrawing *p*-nitro phenyl substituent, exhibit large β value. Similarly, as compared to **3**, the β of other ethenyl increases slightly with increasing the electron donating nature of *p*-phenyl substitution. From previously report on 6-substituted indole based NLO materials, NLO response is also increased with increasing the donor ability of indole moiety through pyrrolidine ring.[47,48] Compounds with weak electron donating or weak electron withdrawing substituent (Cl, OCH_3, OH) (**2**, **4–5**), however, exhibit a low β value as compared to nitro compounds, **1** and **7–9**. The order of β obtained in ethenyl indoles with electron withdrawing group is NO_2 (**1**, **7–9**) > Cl (**2**) > H (**3**) and electron donating OH (**5**) > OCH_3 (**4**) > NH_2 (**6**) (β; **1**: 115, **2**: 20, **3**: 9, **4**: 17, **5**: 24, **6**: 9, **7**: 106, **8**: 43, **9**: 87) (in 10^{-30} esu^{-1} cm^5).

The β value of some of the donor–acceptor nitro compounds, such as *p*-nitro aniline, 4-amino-4′-nitro stilbene, it is shown that the β value is increased from 20 to 100 (in 10^{-30} esu^{-1}, cm^5) with increasing the conjugation length and charge transfer nature of the molecule.[28] From our previous report on thiophene and furan based conjugated compounds, similar results are also found.[45,46] On the other hand, molecule with moderate or weak electron donor/acceptor substituent (cyano, chloro, methoxy, hydroxy), the effect on the β is very small as compared to the nitro substitution.[45,46] For compound **7–9** with *N*-ethyl, *N*-acetyl and *N*-sulfonyl substituent, there is a hindrance in effective π conjugation, which leads to lower β value as compared to **1**. The μ_g for **2–6** is in between 1.05–3.99 debye, whereas μ_g for **1**, **7–9** is 4.34–9.32 debye (Tables S1–S3†). Thus, molecule with charge transfer behavior exhibits large ground state dipole moment, lower optical band gap and larger β value.

Overall, the β value is increased with (i) increasing the dipole moment, (ii) increasing the % of charge transfer behavior (iii) increasing the polarizability and (iv) with increasing the change of excited state dipole moment of 3-substituted indole compounds, whereas β value is decreased with (v) increasing the optical band gap of the molecule. It is the combination of all five factors involved in deciding the NLO response of the molecule. Mostly, for withdrawing substituent, the order of μ_g, μ_e, $\Delta\mu$, π^* and charge separation in 3-substituted indoles is NO_2

(**1**, **7–9**) > Cl (**2**) > H (**3**); and the order of β: NO_2 (**1**, **7–9**) > Cl (**2**) > H (**3**), where as for electron donating substituent, the order of μ_e, $\Delta\mu$, π^* and charge separation is OH (**5**) > OCH_3 (**4**) > NH_2 (**6**); and the order of β: OH (**5**) > OCH_3 (**4**) > NH_2 (**6**). On the other hand higher optical band gap reduced the β value. The order of optical band gap (ΔE) for electron withdrawing substituent: H (**3**) > Cl (**2**) > NO_2 (**1**, **7–9**) and the order of β is NO_2 (**1**, **7–9**) > Cl (**2**) > H (**3**). Similarly, the order ΔE for donating substituent: NH_2 (**6**) > OCH_3 (**4**) > OH (**5**) and the order of β: OH (**5**) > OCH_3 (**4**) > NH_2 (**6**). The optical band gap of *N*-substituted nitro compound (**7–9**) is little larger as compared to **1** and thus, NLO response of **7–9** is slightly lower as compared to compound **1**.

4. Conclusion

In summary, it is shown that the excited state of ethenyl indole is highly sensitive to the solvent and the substituent present on it. Compound **1** and **7–9** with strong electron-attracting substituent exhibits charge transfer and highly dipolar excited state as compared to other ethenyls. Compound **2–6** with a moderate electron donating substituent or weak electron withdrawing or weak electron donating substituent exhibit non polar excited state and insensitive to solvent polarity. The energy band gap of **3** (phenyl ethenyl indole) is decreased by substituting either with an electron withdrawing (Cl, NO_2) or an electron donating (OCH_3, OH, NH_2) substituent at the *p*-phenyl position. The compound with a strong electron accepting, *p*-nitrophenyl ethenyl indole shows 12 times better NLO response as compared to the reference ethenyl indole **3**, whereas, for ethenyls **2–6** bearing a weak or moderately electron withdrawing or electron accepting substituent, exhibit lower NLO response. The β of ethenyl is increased with increasing the order of electron withdrawing nature of phenyl ring. On the other hand, in case of compounds bearing electron donating substituent shows comparable β value. The NLO response is also proportional to the ground state dipole moment, polarizability, dipolar nature and ionic character of the molecule, whereas it is inversely proportional to the optical band gap of the molecule. Overall, the optical properties of indole compound is highly dependent upon the substituent present in phenyl ring and *N*-substitution. In addition, studies on the macroscopic NLO properties of indole compound is an interesting aspect and a future prospective to look into. Thus, the above studies will help in designing and developing optical material for various electronic applications.

Conflicts of interest

There is no conflicts of interest to declare.

Acknowledgements

PKH, JK, NK are thankful to University Grants Commission, New Delhi for research grant (No. F.30-72/2014-BSR) and research fellowship. Authors acknowledged AMRC, IIT Mandi for 1H and 13C NMR facility.

References

1 K. Palczewski, Chemistry and biology of vision, *J. Biol. Chem.*, 2012, **287**, 1612–1619.
2 C. Dugave and L. Demange, Cis-trans isomerisation of organic molecules and biomolecules: implications and applications, *Chem. Rev.*, 2003, **103**, 2475–2532.
3 A. Wand, I. Gdor, J. Zhu, M. Sheves and S. Ruhman, Shedding new light on retinal protein photochemistry, *Annu. Rev. Phys. Chem.*, 2013, **64**, 437–458.
4 A. K. Singh and P. K. Hota, Development of bacteriorhodopsin analogues and studies of charge separated excited states in the photoprocesses of linear polyenes, *Photochem. Photobiol.*, 2007, **83**, 50–62.
5 H. Kobayashi, M. Ogawa, R. Alford, P. L. Choyke and Y. Urano, New strategies for fluorescent probe design in medical diagnostic imaging, *Chem. Rev.*, 2010, **110**, 2620–2640.
6 A. K. Singh and P. K. Hota, Ethenyl indoles as neutral hydrophobic fluorescence probes, *J. Phys. Org. Chem.*, 2007, **20**, 624–629.
7 B.-K. An, J. Gierschner and S. Y. Park, π-Conjugated cyanostilbene derivatives: a unique self-assembly motif for molecular nanostructures with enhanced emission and transport, *Acc. Chem. Res.*, 2012, **45**, 544–554.
8 H. Meir, The photochemistry of stilbenoid compounds and their role in materials technology, *Angew. Chem., Int. Ed. Engl.*, 1992, **31**, 1399–1420.
9 M. Irie, Diarylethenes for memories and switches, *Chem. Rev.*, 2000, **100**, 1685–1716.
10 R. Klajn, Spiropyran-based dynamic materials, *Chem. Soc. Rev.*, 2014, **43**, 148–184.
11 M. Dudek, Z. Pokladek, M. Deiana and K. Matczyszyn, Molecular design and structural characterization of photoresponsive azobenzene-based polyamide units, *Dyes Pigm.*, 2020, **180**, 108501.
12 A. Georgiev, D. Yordanov, D. Dimov, I. Zhivkov, D. Nazarova and M. Weiter, Azomethine phthalimides fluorescent E-Z photoswitches, *J. Photochem. Photobiol., A*, 2020, **393**, 112443.
13 L. Beverina and G. A. Pagani, π-Conjugated zwitterions paradigm of donor-acceptor building blocks in organic based materials, *Acc. Chem. Res.*, 2014, **47**, 319–329.
14 B. Wex and B. R. Kaafarani, Perspective on carbazole-based organic compounds as emitters and hosts in TADF applications, *J. Mater. Chem. C*, 2017, **5**, 8622–8653.
15 H. Hug, M. Bader, P. Mair and T. Glatzel, Biophotovoltaics: natural pigments in dye- sensitized solar cells, *Appl. Energy*, 2014, **115**, 216–225.
16 J. A. Mikroyannidis, D. V. Tsagkournos, S. S. Sharma, Y. K. Vijay and G. D. Sharma, Conjugated small molecules with broad absorption containing pyridine and pyran units: synthesis and application for bulk heterojunction solar cells, *Org. Electron.*, 2010, **11**, 2045–2054.
17 T. Wang, Y. Chen, X. Bao, Z. Du, J. Guo, N. Wang, M. Sun and R. Yang, A new isoindigo-based molecule with ideal energy

levels for solution-processable organic solar cells, *Dyes Pigm.*, 2013, **98**, 11–16.

18 S. Paek, J. K. Lee and J. Ko, Synthesis and photovoltaic characteristics of push–pull organic semiconductors containing an electron-rich dithienosilole bridge for solution-processed small-molecule organic solar cells, *Sol. Energy Mater. Sol. Cells*, 2014, **120**, 209–217.

19 L. Beverina and G. A. Pagani, π-Conjugated zwitterions as paradigm of donor-acceptor building blocks in organic based material, *Acc. Chem. Res.*, 2014, **47**, 319–329.

20 I. Benesperi, H. Michaels and M. Freitag, The researcher's guide to solid-state dye-sensitized solar cells, *J. Mater. Chem. C*, 2018, **6**, 11903–11942.

21 T. Wang, Y. Chen, X. Bao, Z. Du, J. Guo, N. Wang, M. Sun and R. Yang, A new isoindigo based molecule with ideal energy levels for solution processable organic solar cells, *Dyes Pigm.*, 2013, **98**, 11–16.

22 J. K. Lee, B.-S. Jeong, J. Kim, C. Kim and J. Ko, Synthesis and photochemical characterization of fumaronitrile based organic semiconductor and its use in solution processed small molecule organic solar cells, *J. Photochem. Photobiol., A*, 2013, **251**, 25–32.

23 G. D. Sharma, J. A. Mikroyannidis, S. S. Sharma and T. K. R. Justin Thomas, Bulk heterojunction organic photovoltaic devices based on small molecules featuring pyrrole and carbazole and 2-(4-nitrophenyl)acrylonitrile acceptor segments as donor and fullerene derivatives as acceptor, *Dyes Pigm.*, 2012, **94**, 320–329.

24 J. A. Mikroyannidis, D. V. Tsagkournos, S. S. Sharma, Y. K. Vijay and G. D. Sharma, Conjugated small molecules with broad absorption containing pyridine and pyran units: synthesis and application for bulk heterojunction solar cells, *Org. Electron.*, 2010, **11**, 2045–2054.

25 J. Solovjova, T. Malinauskas, M. Daskeviciene, E. Kasparavicius, A. Ilciukaite, A. Sackus, V. Paulauskas and V. Getautis, Triphenylamine-based phenylhydrazone-indolium cationic dyes for solid state DSSC applications, *Mater. Lett.*, 2020, **274**, 128001.

26 *Nonlinear Optical Properties of Organic Molecules and Crystals*, ed. D. S. Chemla and J. Zyss, Academic Press, New York, 1987, vol. 1–2.

27 P. N. Prasad and D. J. Williams, *Introduction to Nonlinear Optical Effects in Molecules and Polymers*, Wiley, New York, 1991.

28 D. R. Kanis, M. A. Ratner and T. J. Marks, Design and construction of molecular assemblies with large second order optical nonlinearities. Quantum chemical aspects, *Chem. Rev.*, 1994, **94**, 195–242.

29 J. Zyss and I. Ledoux, Nonlinear optics in multipolar media: theory and experiments, *Chem. Rev.*, 1994, **94**, 77–105.

30 E. Goovaerts, W. Wenseleers, M. H. Garcia and G. H. Cross, Design and characterization of organic and organometallic molecules for second order nonlinear optics, in *Nonlinear optical materials*, ed. H. S. Nalwa, Academic press, San Diego, CA, 2001, vol. 9, pp. 127–191.

31 S. Boomadevi, H. P. Mittal and R. Dhansekaran, Synthesis, crystal growth and characterization of 3-methyl 4-nitropyridine 1-oxide (POM) single crystal, *J. Cryst. Growth*, 2004, **261**, 55–62.

32 S. R. Forrest and M. E. Thompson, Introduction: organic electronics and optoelectronics, *Chem. Rev.*, 2007, **107**, 923–925.

33 G. S. He, L.-S. Tan, Q. Zheng and P. N. Prasad, Multiphoton absorbing materials: molecular designs, characterizations and applications, *Chem. Rev.*, 2008, **108**, 1245–1330.

34 J. Campo, A. Painelli, F. Terenziani, T. V. Regemorter, D. Beljonne, E. Goovaerts and W. Wenseleers, First hyperpoarizability dispersion of the octupolar molecule crystal violet: multiple resonances and vibrational and solvent effects, *J. Am. Chem. Soc.*, 2010, **132**, 16467–16478.

35 D. Dini, M. J. F. Calvete and M. Hanack, Nonlinear optical materials for the smart filtering of optical radiation, *Chem. Rev.*, 2016, **116**, 13043–13233.

36 L. R. Mingabudinova, V. V. Vinogradov, V. A. Milichko, E. Hey-Hawkins and A. V. Vinogradov, Metal-organic frameworks as competitive materials for non-linear optics, *Chem. Soc. Rev.*, 2016, **45**, 5408–5431.

37 Z. Liu, T. Lu and Q. Chen, An sp-hybridized all-carboatomic ring, cyclo[18]carbon: electronic structure, electronic spectrum and optical nonlinearity, *Carbon*, 2020, **165**, 461–467.

38 M. S. Paley, J. M. Harris, H. Looser, J. C. Baumert, G. C. Bjorklund, D. Jundt and R. J. Twieg, A solvatochromic method for determining second order polarizabilities of organic molecules, *J. Org. Chem.*, 1989, **54**, 3774–3778.

39 C. Bosshard, G. Knopfle, P. Pretre and P. Gunter, Second order polarizabilities of nitropyridine derivatives determined with electric field induced second harmonic generation and a solvatochromic method: a comparative study, *J. Appl. Phys.*, 1992, **71**, 1594–1605.

40 S.-S. P. Chou, G.-T. Hsu and H.-C. Lin, Synthesis and second order nonlinearities of sulfonyl substituted pyrrole imino dyes, *Tetrahedron Lett.*, 1999, **40**, 2157–2160.

41 S. Bruni, E. Cariati, F. Cariati, F. A. Porta, S. Quici and D. Roberto, Determination of the quadratic hyperpolarizability of *trans*-4-[4-(dimethylamino)styryl] pyridine and 5- dimethylamino-1,10-phenanthroline from solvatochromism of absorption and fluorescence spectra: a comparison with electric-field-induced second harmonic generation technique, *Spectrochim. Acta, Part A*, 2001, **57**, 1417–1426.

42 M. E. Reish, A. J. Kay, A. Teshome, I. Asselberghs, K. Clays and K. C. Gordon, Testing computational models of hyperpolarizability in a merocyanine dye using spectroscopic and DFT methods, *J. Phys. Chem. A*, 2012, **116**, 5453–5463.

43 R. V. Solomon, P. Veerapandian, S. A. Vedha and P. Venuvanalingam, Tuning nonlinear optical and optoelectronic properties of vinyl coupled triazene chromophores: a density functional theory and time-dependent density functional theory investigation, *J. Phys. Chem. A*, 2012, **116**, 4667–4677.

44 S. B. Chemate and N. Sekar, Novel iminocoumarin derivatives: synthesis, spectroscopic and computational studies, *J. Fluoresc.*, 2015, **25**, 1615–1628.
45 N. Kumar, M. Paramasivam, J. Kumar, A. Gusain and P. K. Hota, Substituent dependent optical properties of p-phenyl substituted ethenyl-E-thiophene, *J. Fluoresc.*, 2018, **28**, 1207–1216.
46 N. Kumar, M. Paramasivam, J. Kumar, A. Gusain and P. K. Hota, Tuning of optical properties of p-phenyl ethenyl-E-furans: a solvatochromism and density functional theory, *Spectrochim. Acta, Part A*, 2019, **206**, 396–404.
47 J. Liu, M. Zhang, W. Gao, A. A. Fedorchuk and I. V. Kityk, Synthesis and non-linear optical properties of novel conjugated small molecules based on indole donor, *J. Mol. Struct.*, 2018, **1165**, 223–227.
48 M. Zhang, G. Qin, J. Liu, Z. Zhen, A. A. Fedorchuk, G. Lakshminarayana, A. A. Albassam, A. M. El-Naggar, K. Ozga and I. V. Kityk, Modification of indole by electron-rich atoms and their application in novel electron donor materials, *Chem. Phys. Lett.*, 2017, **681**, 105–109.
49 C. Ouyang, J. Liu, Q. Liu, Y. Li, D. Yan, Q. Wang, M. Guo and A. Cao, Preparation of main- chain polymers based on novel monomers with D-pi-a structure for application in organic second-order nonlinear optical materials with good long-term stability, *ACS Appl. Mater. Interfaces*, 2017, **9**, 10366–10370.
50 J. Kumar, N. Kumar, N. Sati and P. K. Hota, Antioxidant properties of ethenyl indole: DPPH assay and TDDFT studies, *New J. Chem.*, 2020, **44**, 8960–8970.
51 A. K. Singh and P. K. Hota, Fluorescence and photoisomerization studies of *p*-nitrophenyl substituted indolic ethenes, *J. Phys. Org. Chem.*, 2006, **19**, 43–52.
52 E. Wenkert, J. H. Udelhofen and N. K. Bhattacharyya, 3-Hydroxy methyleneoxindole and its derivatives, *J. Am. Chem. Soc.*, 1959, **81**, 3763–3768.
53 G. F. Smith, Indoles. Part I. The formylation of indole and some reactions of 3-formyl indole, *J. Chem. Soc. Part IV*, 1954, 3842–3846.
54 D. Nagarathnam, A facile synthesis of 3-substituted indoles, *J. Heterocycl. Chem.*, 1992, **29**, 953–958.
55 E. G. McRae, Theory of solvent effects on molecular electronic spectra, frequency shifts, *J. Phys. Chem.*, 1957, **61**, 562–572.
56 C. Reichardt, Solvatochromic dyes as solvent polarity indicators, *Chem. Rev.*, 1994, **94**, 2319–2358.
57 C. Reichardt, *Solvents and solvent effects in organic chemistry*, VCH, Weinheim, Basel, Germany, 2nd edn, 1990, ch. 6, pp. 285–338.
58 N. Kumar, J. Kumar and P. K. Hota, Substituent dependence charge transfer and photochemical properties of donor-acceptor substituted ethenyl thiophenes, *J. Fluoresc.*, 2017, **27**, 1729–1738.
59 J. L. Oudar and D. S. Chemla, Hyperpolarizabilities of the nitroanilines and their relations to the excited state dipole moment, *J. Chem. Phys.*, 1977, **66**, 2664.
60 J. B. Birks, *Photophysics of Aromatic Molecules*, Wiley-Interscience, London, 1970.
61 F. Neese, The ORCA program system, *Wiley Interdiscip. Rev.: Comput. Mol. Sci.*, 2012, **2**, 73–78.
62 T. Petrenko and F. Neese, A general efficient quantum chemical method for predicting absorption bandshapes, resonance raman spectra and excitation profiles for larger molecules, *J. Chem. Phys.*, 2007, **127**, 164319.
63 T. Petrenko, O. Krylova, F. Neese and M. Sokolowski, Optical absorption and emission properties of rubrene: insight by a combined experimental and theoretical study, *New J. Phys.*, 2009, **11**, 015001.
64 A. Dreuw and M. Head-Gordon, Single reference ab initio methods for the calculation of excited states of large molecules, *Chem. Rev.*, 2005, **105**, 4009–4037.
65 J. Kulhánek, F. Bureš, A. Wojciechowski, M. Makowska-Janusik, E. Gondek and I. V. Kityk, Optical operation by chromophores featuring 4,5-dicyanoimidazole embedded within poly(methyl methacrylate) matrices, *J. Phys. Chem. A*, 2010, **114**, 9440–9446.
66 T. Yanai, D. P. Tew and N. C. Handy, A new hybrid exchange–correlation functional using the coulomb-attenuating method (CAM-B3LYP), *Chem. Phys. Lett.*, 2004, **393**, 51–57.
67 F. Weigend and R. Ahlrichs, Balance basis sets of split valence, triple zeta valence and quadruple zeta valence quality for H to Rn: design and assessment of accuracy, *Phys. Chem. Chem. Phys.*, 2005, **7**, 3297–3305.
68 B. S. Neporent and N. G. Bakhshiev, On the role of universal and specific intermolecular interactions in the influence of the solvent on the electronic spectra of molecules, *Opt. Spectrosc.*, 1960, **8**, 408–413.
69 C. Reichardt, S. Lobbecke, A. M. Mehranpour and G. Schafer, Pyridinium N-Phenoxide betaines and their application to the determination of solvent polarities synthesis and Uv-visible spectroscopic properties of new lipophillic *tert*-butyl- and 1-adamantyl substituted, negatively solvatochromic pyridinium N-Phenolate betaine dyes, *Can. J. Chem.*, 1998, **76**, 686–694.
70 M. B. Smith and J. March, in *March's Advanced organic chemistry, reactions, mechanism, and structure*, ed. M. B. Smith, A wiley-interscience publication, New York, 6th edn, 2007.
71 M. J. Kamlet, J.-L. M. Abboud and R. W. Taft, The solvatochromic comparison method. 6. The π^* scale of solvent polarities, *J. Am. Chem. Soc.*, 1977, **99**, 6027–6038.
72 A. K. Singh and P. K. Hota, Photoreactivity of donor-acceptor ethenes, *Indian J. Chem., Sect. B: Org. Chem. Incl. Med. Chem.*, 2003, **42**, 2048–2053.
73 A. K. Singh and P. K. Hota, Absorption and fluorescence spectral properties of donor acceptor ethenes bearing indole and *p*-nitrophenyl substituents, *Res. Chem. Intermed.*, 2005, **31**, 85–101.
74 Y. Sonoda, Y. Shimoi, M. Goto, N. Tohnai and M. Kanesato, Fluorescence properties of (E,E,E)-1,6-di(n-naphthyl)-1,3,5-hexatriene (n = 1, 2): effects of internal rotation, *J. Phys. Chem. A*, 2013, **117**, 566–578.

75 C. Singh, R. Ghosh, J. A. Mondal and D. K. Palit, Excited state dynamics of a push-pull stilbene: a femtosecond transient absorption spectroscopic study, *J. Photochem. Photobiol., A*, 2013, **263**, 50–60.

76 C.-K. Lin, Y.-F. Wang, Y.-C. Cheng and J.-S. Yang, Multisite constrained model of *trans*-4-(N,N-dimethylamino)-4-nitrostilbene for structural elucidation of radiative and nonradiative excited states, *J. Phys. Chem. A*, 2013, **117**, 3158–3164.

77 N. Kumar, J. Kumar and P. K. Hota, Substituent dependent photoreactivity of donor-acceptor phenyl ethene, *Lett. Org. Chem.*, 2018, **15**, 479–484.

78 J. Kumar, N. Kumar and P. K. Hota, Excited state and fluorescence probe properties of donor-acceptor substituted ethenes: a plausible photochromic material for organic electronics, *Indian J. Chem., Sect. B: Org. Chem. Incl. Med. Chem.*, 2018, **57**, 301–307.

79 P. K. Hota and A. K. Singh, Donor-acceptor conjugated linear polyenes: a study of excited state intramolecular charge transfer, photoisomerisation and fluorescence probe properties, *J. Fluoresc.*, 2018, **28**, 21–28.